Engineering Technology Open Access Journal

Juniper Publishers key to the Researchers

Research Article
Volume 3 Issue 4 - November 2020
DOI: 10.19080/ETOAJ.2020.03.555620

Eng Technol Open Acc

A Water Absorption Model Based on Self-Consistent Theory for Solid Buoyancy Materials

Jingze Wang[1,2,3] and Weicheng Cu[i2,3]*

[1]*Institute of Advanced Technology, Westlake Institute for Advanced Study, China*

[2]*School of Engineering, Westlake University, China*

[3]*Key Laboratory of Coastal Environment and Resources Research of Zhejiang Province, Westlake Institute for Advanced Study, China*

Submission: November 11, 2020; **Published:** November 27, 2020

***Corresponding author:** Weicheng Cui, School of Engineering, Westlake University & Key Laboratory of Coastal Environment and Resources Research of Zhejiang Province, Institute of Advanced Technology, Westlake Institute for Advanced Study, 18 Shilongshan Road, Hangzhou 310024, China

Abstract

The water absorption of solid buoyancy material seriously endangers the safety and usability of deep manned/unmanned submersibles. However, the theoretical models which can accurately predict the compressive strength and water absorption of solid buoyancy materials have not been found yet. This seriously hinders the safe operation of deep manned/unmanned submersibles. Therefore, a comprehensive experimental and numerical study is carried out on the solid buoyancy materials used in full ocean depth submersibles. In this paper, a water absorption model according to self-consistent theory for solid buoyancy materials is proposed. Then the water absorption model is verified by comparing with the experimental data. The model shows that the water absorption behavior can be divided into two stages. In the first stage, the water absorption is directly proportional to the volume fraction of fractured hollow glass beads, while in the second stage, the relationship becomes exponential due to the fragmentation propagation of hollow glass beads.

Keywords: Deep sea submersible; Buoyancy material; Compressive strength; Water absorption; Crack propagation

Introduction

Solid buoyancy material is one of the key technologies in submersible development [1-3]. Its importance in deep sea exploration has been widely recognized [4-7]. In the operation of the full ocean depth manned/unmanned submersibles, the issue how to check the status of the buoyancy material becomes one of the main obstacles because that buoyancy materials fully satisfied the classification society rule requirement of 1.5 safety factor do not exist[1]. There are two hazards which come from the water absorption of solid buoyancy material to the safety and reliability of deep manned/unmanned submersibles [8]. The first is reduction of compressive strength of solid buoyancy materials. The water absorption causes the hydrolysis and swelling of epoxy resin, which reduces the bonding strength of hollow glass beads and epoxy resin [9-12]. Then the compressive strength of solid buoyancy material is reduced, which endangers the safety of deep manned/unmanned submersibles. The second is that it reduces the ability of solid buoyancy materials providing buoyancy compensation. Water absorption increases the density of solid buoyancy materials [8], which reduces the abilities of deep manned/unmanned submersibles to float and dive. Therefore, studying the water absorption behavior of solid buoyancy materials is very important in submersible design and operation.

Solid buoyancy materials are usually used in deep sea environment [13,14]. The hollow glass beads fracture under water pressure. At this moment, the solid buoyancy material can be regarded as a porous medium after the hollow glass beads fracturing. It means that the water absorption behavior of solid buoyancy materials is mainly caused by the fractured hollow glass beads. However, previous researchers mainly focused on how the volu Figure me fraction [15-17], compressive strength [18], ratio of wall thickness to radius [19-21] and density [22] of hollow glass beads influence the failure behavior of solid buoyancy materials. The compressive strength model for solid buoyancy materials has not been found. Liang has done some researches on the fracture behavior of hollow glass beads [23-26]. However, these hollow glass beads are not used in solid buoyancy materials. Only two papers focusing on the water absorption of solid buoyancy materials have been found [8,27]. These two papers mainly

investigated the influencing factors of water absorption behavior. The effect of fractured hollow glass bead on the water absorption behavior of solid buoyancy materials has not been recognized. The theoretical model which can accurately predict the water absorption has not been found yet. The difficulties in proposing a model come from the randomness of particle size and spatial distributions and the complexities of crack propagation in multi-phase and multi-scale.

In this paper, based on the self-consistent theory, a water absorption model for the solid buoyancy materials is proposed. Then the water absorption model is verified by comparing with the experimental data. The theoretical model shows that the water absorption behavior of solid buoyancy materials can be divided into two stages. In the first stage, the water absorption is directly proportional to the volume fraction of fractured hollow glass beads, while in the second stage, the relationship becomes exponential due to the fragmentation propagation of hollow glass beads.

Theoretical Derivation

Basic assumptions

In order to build the mathematical model, the following six assumptions for epoxy resin, glass beads and the buoyancy failure mode are made:

a) The hollow glass beads and the epoxy resin are isotropic and homogeneous.

b) The main failure mode of full ocean depth solid buoyancy materials is the fragmentation of hollow glass beads. The water absorption behavior of solid buoyancy materials is mainly caused by the fractured hollow glass beads.

c) The particle sizes of hollow glass beads follow a normal distribution.

d) The density of all hollow glass beads of identical types is a constant that is independent of particle size.

e) The failure of hollow glass beads under uniform pressure is similar to a mode-II failure.

f) It is difficult to characterize the shapes and sizes of the initial defects in hollow glass beads. Therefore, it is assumed that there is an average value to represent the effect of initial defects on the compressive strength of hollow glass beads.

The compressive strength distribution model

In this section, a unit cell is assumed to be wrapped in a medium large enough in deep sea environment. If the medium is isotropic and homogeneous and its properties are the same as solid buoyancy material. Then the stress at anywhere in the medium is equal to the water pressure it bears. This means that the pressure on the surface of concentric spherical shell is also equal to the water pressure. At this time, the stresses in the unit cell wrapped by the medium is similar to that in the unit cell of solid buoyancy material.

According to the elastic theory, the stresses and strains at the interface between hollow glass bead and epoxy resin should follow the stress balance and displacement coordination conditions. Therefore, there are:

$$\begin{cases} \sigma_{r_g} = \sigma_{r_m} \\ \varepsilon_{Tm} = \varepsilon_{Tg} \end{cases} \tag{1}$$

Where, σ_{r_g} and σ_{r_m} are the radial stresses in hollow glass bead and epoxy resin, respectively. ε_{Tg} and ε_{Tm} are the tangential strains of hollow glass bead and epoxy resin at their interface, respectively.

In the unit cell, the internal pressure of the hollow glass bead is 0. According to the elastic theory, the radial and tangential normal stresses in spherical shell under a uniform load is as follows:

$$\begin{cases} \sigma_{r_g} = -\dfrac{1-\dfrac{r_g^3}{r^3}}{1-\dfrac{r_g^3}{r_i^3}}\sigma_{r_i} \\ \sigma_{T_g} = -\dfrac{1+\dfrac{r_g^3}{2r^3}}{1-\dfrac{r_g^3}{r_i^3}}\sigma_{r_i} \end{cases} \quad (r_g \le r \le r_i) \tag{2}$$

Where, σ_{T_g} is the tangential stress in the hollow glass bead. σ_{r_i} is the radial stress at the interface. r_g is the inner radius of the hollow glass bead. r_i is the radius of interface. r is a parameter in Eq. (2) ranges from r_g to r_i. Unlike the hollow glass bead, the thin shell made of epoxy resin bears internal and external pressures. Therefore, the radial and tangential normal stresses distribute as follows:

$$\begin{cases} \sigma_{r_m} = -\dfrac{\dfrac{r_m^3}{r^3}-1}{\dfrac{r_m^3}{r_i^3}-1}\sigma_{r_i} - \dfrac{1-\dfrac{r_i^3}{r^3}}{1-\dfrac{r_i^3}{r_m^3}}p \\ \sigma_{T_m} = \dfrac{\dfrac{r_m^3}{2r^3}+1}{\dfrac{r_m^3}{r_i^3}-1}\sigma_{r_i} - \dfrac{1+\dfrac{r_i^3}{2r^3}}{1-\dfrac{r_i^3}{r_m^3}}p \end{cases} \quad (r_i \le r \le r_m) \tag{3}$$

Where, σ_{T_m} is the tangential stress in the epoxy resin. r_m is the outer radius of the epoxy resin. r is a parameter in Eq. (3) ranges from r_i to r_m. p is the uniform pressure on the surface of unit cell. Substituting $r = r_i$ into Eq. (2) and Eq. (3) yields:

$$\sigma_{r_g} = \sigma_{r_m} = -\sigma_{r_i} \tag{4}$$

$$\begin{cases} G_p = -\dfrac{1+\dfrac{r_g^3}{2r_i^3}}{1-\dfrac{r_g^3}{r_i^3}} = -\dfrac{1+\dfrac{V_h}{2}}{1-V_h} \\ M_p = \dfrac{\dfrac{r_m^3}{2r_i^3}+1}{\dfrac{r_m^3}{r_i^3}-1} = \dfrac{1+2V_g}{2(1-V_g)} \\ M_0 = \dfrac{3}{2\left(1-\dfrac{r_i^3}{r_m^3}\right)} = \dfrac{3}{2(1-V_g)} \end{cases} \tag{5}$$

How to cite this article: Jingze W, Weicheng C. A Water Absorption Model Based on Self-Consistent Theory for Solid Buoyancy Materials. Eng Technol Open Acc. 2020; 3(4): 555620. DOI: 10.19080/ETOAJ.2020.03.555620.

Eq. (4) shows that the stress balance condition at the interface is automatically satisfied. Aiming to simplify the calculation process, several parameters are defined:

Where, $V_h = \frac{r_g^3}{r_i^3}$ is the hollowness of the glass bead. While $V_g = \frac{r_i^3}{r_m^3}$ is the volume fraction of hollow glass bead in the unit cell. Substituting $r = r_i$ and Eq. (5) into Eq. (2) and Eq. (3) yields the tangential normal stresses of hollow glass bead and epoxy resin:

$$\begin{cases} \sigma_{T_g} = G_p \sigma_{r_i} \\ \sigma_{T_m} = M_p \sigma_{r_i} - M_0 p \end{cases} \quad (r = r_i) \qquad (6)$$

Both hollow glass bead and epoxy resin in the unit cell are isotropic materials. Therefore, the tangential normal strains of hollow glass bead and epoxy resin at their interface are:

$$\begin{cases} \varepsilon_{T_g} = \frac{1}{E_g}\left[(1-\mu_g)\sigma_{T_g} - \mu_g \sigma_{r_g}\right] \\ \varepsilon_{T_m} = \frac{1}{E_m}\left[(1-\mu_m)\sigma_{T_m} - \mu_m \sigma_{r_m}\right] \end{cases} \qquad (7)$$

Where, E_g and E_m are the elastic modulus of hollow glass bead and epoxy resin, respectively. μ_g and μ_m are the Poisson's ratios of hollow glass bead and epoxy resin, respectively. According to Eq. (1), the tangential normal strains of hollow glass bead and epoxy resin are equal at the interface. Substituting Eq. (6) and Eq. (7) into Eq. (1) yields the radial normal stress at the interface:

$$\sigma_{r_i} = \frac{(1-\mu_m)M_0 p}{\left[(1-\mu_m)M_p + \mu_m\right] - \frac{E_m}{E_g}\left[(1-\mu_g)G_p + \mu_g\right]} \qquad (8)$$

Substituting Eq. (8) into Eq. (2) yields the radial and tangential normal stresses in the hollow glass bead. Now, we can obtain the radial distribution of the maximum shear stress in the hollow glass bead:

$$\tau_{\max} = \frac{\sigma_{r_g} - \sigma_{T_g}}{2} = \frac{3}{4}\left(\frac{\frac{r_g^3}{r^3}}{1-\frac{r_g^3}{r_i^3}}\right)\sigma_{r_i} \quad (r_g \le r \le r_i) \qquad (9)$$

Obviously, when $r = a$, the maximum shear stress is the maximum. It means that the crack source will occur on the inner surface of hollow glass beads in the unit cell. Substituting Eq. (5) and Eq. (8) into Eq. (9) yields the fracture strength of the unit cell:

$$\tau_{th} = \frac{9}{8}\frac{1}{(1-V_h)(1-V_g)}\frac{p}{\left[\frac{1+2V_g}{2(1-V_g)} + \frac{\mu_m}{(1-\mu_m)}\right] - \frac{E_m}{E_g}\left[\frac{2(\mu_g-1)-V_h(\mu_g+1)}{2(1-\mu_m)(1-V_h)}\right]} \qquad (10)$$

Where, τ_{th} is the shear strength of the unit cell.

Griffith proposed a theoretical expression of the crystal fracture strength for crystal materials:

$$\sigma_{th} = \sqrt{\frac{E\gamma}{b}} \qquad (11)$$

where E is the elastic modulus of the material, b is the equilibrium lattice constant, and γ is the surface energy. Eq. (11) shows that the fracture strength of crystal materials is proportional to the square root of surface energy, while the surface energy increases with the specific surface area [28-29]. The force, displacement and modulus in Eq. (11) are generalized quantities. Therefore, the fracture strength of solid materials under shear stress is assumed to be proportional to the square root of surface energy:

$$\tau_{th} \propto \sqrt{\gamma} \qquad (12)$$

Hollow glass beads are spherical shell structures, but compared to the parameters of hollow glass beads, it is more reasonable to regard hollow glass beads as solid spheres when calculating the specific surface area. Therefore, the specific surface areas are:

$$\gamma \propto \frac{4\pi r^2}{\frac{4}{3}\pi r^3} = \frac{3}{r} \qquad (13)$$

According to Eq. (12) and Eq. (13), the fracture strength under shear stress is inversely proportional to the root of the radius. We define k as a proportional constant, and we obtain:

$$\tau_{th} = \frac{k}{\sqrt{r}} \qquad (14)$$

Substituting Eq. (14) into Eq. (10) and transposing it yields the failure pressure of the hollow glass bead:

$$p_{th} = \frac{8(1-V_h)(1-V_g)}{9}\left\{\left[\frac{1+2V_g}{2(1-V_g)} + \frac{\mu_m}{(1-\mu_m)}\right] - \frac{E_m}{E_g}\left[\frac{2(\mu_g-1)-V_h(\mu_g+1)}{2(1-\mu_m)(1-V_h)}\right]\right\}\frac{k}{\sqrt{r}} \qquad (15)$$

Defining a parameter K_{III} whose expression is:

$$K = \frac{8(1-V_h)(1-V_g)}{9}\left\{\left[\frac{1+2V_g}{2(1-V_g)} + \frac{\mu_m}{(1-\mu_m)}\right] - \frac{E_m}{E_g}\left[\frac{2(\mu_g-1)-V_h(\mu_g+1)}{2(1-\mu_m)(1-V_h)}\right]\right\}k \qquad (16)$$

Then Eq. (15) can be simplified as:

$$p_{th} = \frac{K}{\sqrt{r}} \qquad (17)$$

Eq. (17) expresses the failure pressure of the unit cell. The compressive strength probability density function and distribution function of the buoyancy material are:

$$\begin{cases} f(p_{th}) = \frac{1}{\sigma}\sqrt{\frac{2}{\pi}}\frac{K^2}{p_{th}^3}\exp\left(-\frac{\left[\left(\frac{K}{p_{th}}\right)^2 - \mu\right]^2}{2\sigma^2}\right) \\ F(p_{th}) = \frac{K^2}{\sigma}\sqrt{\frac{2}{\pi}}\int_{\frac{K}{\sqrt{r_{\max}}}}^{p_{th}}\frac{1}{p_{th}^3}\exp\left[-\frac{\left(\left(\frac{K}{p_{th}}\right)^2 - \mu\right)^2}{2\sigma^2}\right]dp_{th} \end{cases} \qquad (18)$$

Where, p_{th} is the uniform pressure when the unit cell cracks. μ and σ are the average and standard deviation of the outer radius for the hollow glass bread.

The water absorption model

According to Eq. (17), the radius range of fractured hollow glass beads under a certain water pressure can be known. Then, according to the radius, the volume fraction of the fractured hollow glass beads can be calculated. Based on the assumption about the relationship between the water absorption of solid buoyancy material and the volume fraction of fractured hollow glass beads, the water absorption caused by fractured hollow glass beads can be obtained. According to the relationship between the radius and volume of the spherical shell, there is:

How to cite this article: Jingze W, Weicheng C. A Water Absorption Model Based on Self-Consistent Theory for Solid Buoyancy Materials. Eng Technol Open Acc. 2020; 3(4): 555620. DOI: 10.19080/ETOAJ.2020.03.555620.

$$V=\frac{4}{3}\pi r^3$$

$$\Rightarrow r=\left(\frac{3V}{4\pi}\right)^{\frac{1}{3}} \quad (19)$$

$$\Rightarrow \frac{dr}{dV}=\frac{1}{4\pi}\left(\frac{3V}{4\pi}\right)^{-\frac{2}{3}}$$

Substituting Eq. (19) into the probability integral formula of normal distribution yields:

$$F(V_{th})=\frac{1}{4\pi\sigma\sqrt{2\pi}}\int_{V_{min}}^{V_{th}}\left(\frac{3V_{th}}{4\pi}\right)^{-\frac{2}{3}}\exp\left[-\frac{\left(\left(\frac{3V_{th}}{4\pi}\right)^{\frac{1}{3}}-\mu\right)^2}{2\sigma^2}\right]dV_{th}$$

$$\Rightarrow f(V_{th})=\frac{1}{4\pi\sigma\sqrt{2\pi}}\left(\frac{3V_{th}}{4\pi}\right)^{-\frac{2}{3}}\exp\left[-\frac{\left(\left(\frac{3V_{th}}{4\pi}\right)^{\frac{1}{3}}-\mu\right)^2}{2\sigma^2}\right] \quad (20)$$

The probability distribution function and probability density function of hollow glass bead volume is shown in Eq. (20). It should be noted that $F(V_{th})$ is the probability of the remaining hollow glass beads. Therefore, the probability of fractured hollow glass beads is $1-F(V_{th})$. The volume fraction of the fractured hollow glass beads is:

$$V_g(p_{th})=\left[1-F(V_{th})\right]V_g \quad (21)$$

After the fragmentations, only the hollow part of glass beads can absorb water. The volume fraction of the hollow part is

$$V_g(p_{th})=\left[1-F(V_{th})\right]V_g \quad (22)$$

If the hollow part of the fractured glass beads can be completely filled with water, then the water absorption caused by fractured hollow glass beads is:

$$M_s=\frac{\rho_w}{\rho_s}\left[1-F(V_{th})\right]V_gV_h \quad (23)$$

Where, ρ_s and ρ_w are the densities of solid buoyancy material and water, respectively. The hollowness V_h is usually an unknown parameter. Substituting $V_h=1-\frac{\rho_g}{\rho_b}$ into Eq. (23) yields:

$$M_s=\frac{\rho_w}{\rho_s}\left(1-\frac{\rho_g}{\rho_b}\right)\left[1-F(V_{th})\right]V_g \quad (24)$$

It is assumed that the water absorption behavior of solid buoyancy materials can be divided into two stages. In the first stage, the water pressure is still low. The crack does not propagate after the hollow glass beads fracturing. On the other hand, due to the short time of testing time, the hollow part of the fractured glass beads cannot be completely filled with water. Therefore, it is assumed that the water absorption is directly proportional to the volume fraction of fractured hollow glass beads. In the second stage, the fragmentations of hollow glass beads propagate under a certain water pressure. Then the water absorption is exponentially related to the volume fraction of the fractured hollow glass beads. Based on these assumptions, the water absorption model for the solid buoyancy material is:

$$M=\begin{cases}k'\frac{\rho_w}{\rho_s}\left(1-\frac{\rho_g}{\rho_b}\right)\left[1-F(V_{th})\right]V_g & p\le p_0\\ k'a^{p-p_0}\frac{\rho_w}{\rho_s}\left(1-\frac{\rho_g}{\rho_b}\right)\left[1-F(V_{th})\right]V_g & p>p_0\end{cases} \quad (25)$$

Where, k' is a proportional constant. It represents the ratio of water absorption to the volume fraction of the hollow part of the fractured glass beads. p_0 is a certain water pressure which is the boundary between the first and the second stages.

Model Verification

Experimental objects and results

In this section, some water absorption experiments have been done to verify the water absorption model for the solid buoyancy material. The test object is HZ-42 solid buoyancy material produced by "ESS" company (Engineered Syntactic Systems). For this solid buoyancy material, the volume fraction of epoxy resin is 0.3. The density is 0.67±0.3g/cm^3. There are 3 kinds of samples which numbered E1, E2 and E3, respectively. The quantities of E1, E2 and E3 are 4, 3 and 3, respectively. The size of E1 is 610mm×305mm×100mm. The sizes of E2 and E3 are 305mm×305mm×100mm. Six groups of water pressure experiments have been done. The test object, water pressure and holding time in every experiment are given in Table 1. The processes of water pressure experiment are as follows:

Table 1: The test objects, water pressures and holding times.

Group	Test Objects	Water Pressure (MPa)	Holding Time (h)
1st	E1, E2, E3	115	2h
2nd	E1	126.5	2h
3rd	E1, E3	143.8	2h
4th	E2	145	2h
5th	E2, E3	160	2h
6th	E1	165	2h

a) Weigh the masses of solid buoyancy material samples by electronic balance (in gram). Then measure the volumes of the solid buoyancy material samples by drainage method.

b) Place the solid buoyancy material samples in a 180MPa pressure chamber after counterweighing. Then check the relevant equipment and prepare for the pressure test.

c) The pressure is uniformly pressurized to the test water pressure at a rate of 2-3MPa/min. Then after holding for two hours, the water pressure is released to 0MPa at a rate of 2-3MPa/min.

How to cite this article: Jingze W, Weicheng C. A Water Absorption Model Based on Self-Consistent Theory for Solid Buoyancy Materials. Eng Technol Open Acc. 2020; 3(4): 555620. DOI: 10.19080/ETOAJ.2020.03.555620.

d) After completion of test, take out the buoyancy samples as soon as possible. Investigate the surface. Then dry the sample surfaces with absorbent paper. Weigh the masses of samples again. The whole process should be completed within 15 minutes.

It is shown that small cracks appear on the solid buoyancy material surface under 160MPa pressure. While obvious cracks appear on the surface of samples under 165MPa pressure. The water absorptions tested in these experiments are shown in Table 2. It shows that the water absorptions remain at a very low level before 145MPa. While they increased rapidly after 160MPa.

Table 2: The water absorptions of solid buoyancy materials (%).

Samples	115.0MPa	126.5MPa	143.8MPa	145.0MPa	160.0MPa	165.0MPa
E-1	0.00797	0.01195	0.01036	\	\	1.593
E-2	0.01441	\	\	0.0096	1.012	\
E-3	0.01123	\	0.0161	\	0.3146	\

Verification of theoretical models

In this section, the water absorption model is verified by comparing with the experimental results. The material properties of hollow glass beads and epoxy resin have been tested. The results show that the properties of hollow glass beads are similar to that of im16K. The material parameters of im16K and epoxy resin are shown in Table 3. The size distributions, densities, compressive strengths and other parameters of im16K in Table 4 were provided by a representative of 3M. The hollow glass beads with radius of [2~14μm] are selected as the research objects. According to the calculation, the proportion of hollow glass beads in this range is $P\{2 \le r \le 14\} = 99.988\%$.

According to the uniform pressure under which 90% of im16k remain intact (see Table 4), by looking up the cumulative probability function table of standard normal distribution, we yields $k = 39.20MPa \cdot mm^{\frac{1}{2}}$. Then, Substituting the value of k and other material parameters shown in Table 3 into Eq. (16) yields $K = 13.5MPa \cdot mm^{\frac{1}{2}}$.

The relationship between the compressive strength of unit cell and the radius of hollow glass bead is shown in Figure 1. It shows that the compressive strengths of the unit cells decrease with the radii of hollow glass bead increasing.

t3 t4f

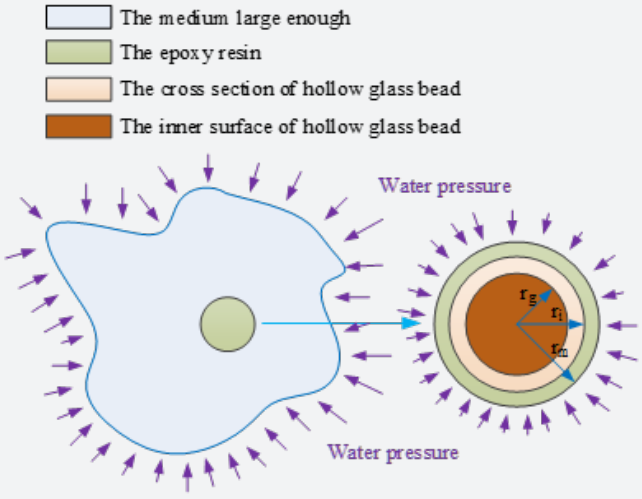

Figure 1: The unit cell model based on self-consistent theory.

Table 3: The material parameters.

Objects	Young's Modulus (GPa)	Poisson's Ratio	Density (g/cm^3)	Compressive Strength (MPa)
Epoxy resin	4.5	0.35	1.18	180
Glass	60	0.23	2.18	\
im6K	\	\	0.46	\

How to cite this article: Jingze W, Weicheng C. A Water Absorption Model Based on Self-Consistent Theory for Solid Buoyancy Materials. Eng Technol Open Acc. 2020; 3(4): 555620. DOI: 10.19080/ETOAJ.2020.03.555620.

Table 4: The parameters of im16K.

Kinds	Density (g/cm³)	Particle Size (μm)			Strength of 90% retention (MPa)
		10th	50th	90th	
im16K	0.46	12	20	20	110.32

The radius range of the fractured hollow glass beads under a certain water pressure can be obtained according to Figure 2. Then volume fractions of the fractured hollow glass beads can be calculated. Taking 115.0MPa as an example, the radius of the fractured hollow glass beads is 10.00μm. The corresponding volume is 4188.79μm³. The radii and volumes under other pressures are shown in Table 5.

Table 5: The corresponding radii and volumes under the water pressures.

Water pressures (MPa)	115	126.5	143.8	145	160	165
Radii (μm)	10	8.3	6.4	6.3	5.2	4.9
Volumes (μm³)	4188.79	2395.1	1098.07	1047.39	588.98	492.81

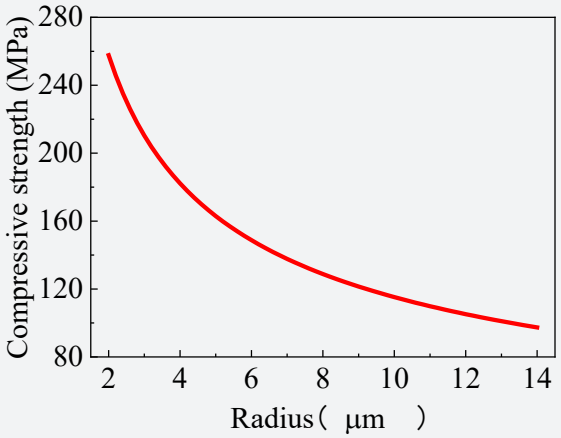

Figure 2: The relationship between the compressive strengths of the unit cells and the radii of hollow glass beads.

The volume probability density distribution and cumulative probability distribution of hollow glass beads are shown in Figure 3. It shows that the probability density is asymmetrically distributed. Therefore, it does not follow the normal distribution. The volume fraction of fractured hollow glass beads can be obtained according to the cumulative probability distribution.

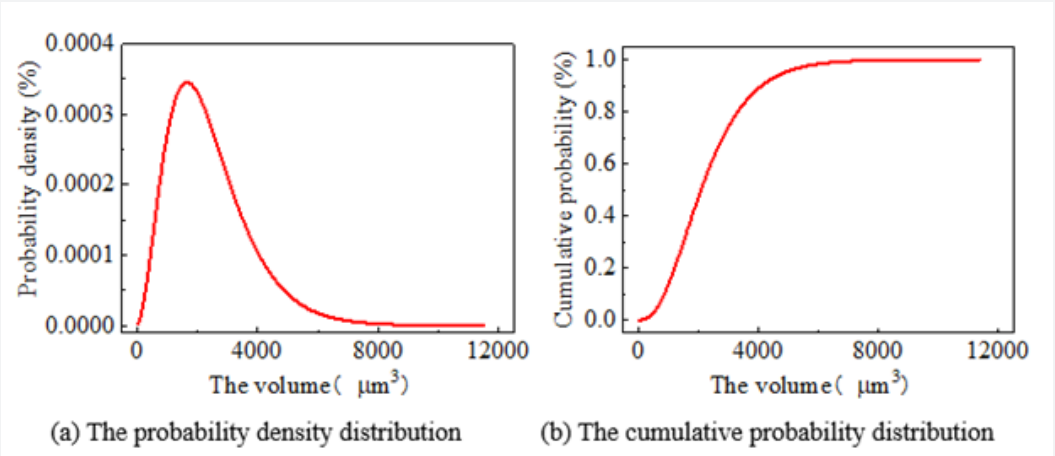

Figure 3: The volume distributions of the unit cells.

How to cite this article: Jingze W, Weicheng C. A Water Absorption Model Based on Self-Consistent Theory for Solid Buoyancy Materials. Eng Technol Open Acc. 2020; 3(4): 555620. DOI: 10.19080/ETOAJ.2020.03.555620.

The water absorption caused by fractured hollow glass beads can be obtained referring to the calculation process from Eq. (21) to Eq. (24). The probability and the volume fraction of the fractured hollow glass beads, the volume fraction of the hollow part, water absorption caused by the fractured glass beads fragmentation are given in Table 6. Compared with the experimental data in Table 2, the unknown parameters in Eq. (25) can be obtained and listed in Eq. (26).

$$\begin{cases} \mu = 0.008 \\ \sigma = 0.00156 \\ k' = 0.0015 \\ a = 1.0734 \\ p_0 = 128.4 \end{cases} \quad (26)$$

Table 6: The calculation process of water absorption.

Water pressures (MPa)	115	126.5	143.8	145	160	165
The probability of the fractured hollow glass beads (%)	9.45	41.13	83.99	85.5	96.11	97.48
The volume fraction of the fractured hollow glass beads (%)	6.61	28.79	58.79	59.85	67.28	68.23
The volume fraction of the hollow part (%)	7.45	32.45	66.26	67.46	75.83	76.91
The water absorption caused by the fractured glass beads (%)	7.67	33.41	68.21	69.44	78.06	79.17

Substituting Eq. (26) into Eq. (25) yields the water absorption model of solid buoyancy materials. Comparison between theoretical values and experimental results is shown in Figure 4. It can be seen that the theoretical values agree with the experimental data very well. This verified the theoretical model. The model shows that 128.4MPa is a certain water pressure after which the water absorption is exponentially related to the volume fraction of the fractured hollow glass beads. It means that the fractured hollow glass bead will become the source and then cause crack propagation under this water pressure.

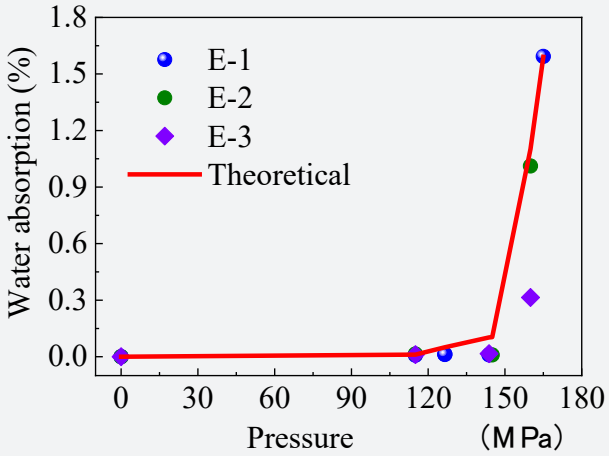

Figure 4: Comparison between theoretical values and experimental data.

Analysis

Deviation analysis

The probability of fractured hollow glass beads in Table 6 is 97.48% under 165MPa. Experimental results show that the solid buoyancy materials do not fail so serious. This deviation may mainly come from the volume fraction change during the fracture process of hollow glass beads. With hollow glass beads fracturing, the volume fraction of epoxy resin increases (see Figure 5). This makes the epoxy resin to share more pressure which is significant to alleviate the fracture of hollow glass beads. However, simply introducing the volume fraction increase of epoxy resin into the derivation process may be inconsistent with the fact. Therefore, to study how the volume fraction change of epoxy resin influences the fracture of hollow glass beads, further study is required.

Stress distributions

An im16K hollow glass bead with a radius of 8μm is selected as the research object in this section. The inner radius of hollow glass bead and the outer radius of unit cell can be obtained according to the hollow degree and the volume fraction of hollow glass beads. The uniform pressure and the sizes of unit cell are shown in Table 7.

The radial and tangential normal stress distributions along radial direction are shown in Figure 6. It can be seen that most of the radial and tangential normal stresses are borne by the hollow glass bead. Figure 6(b) shows that the tangential normal stress

How to cite this article: Jingze W, Weicheng C. A Water Absorption Model Based on Self-Consistent Theory for Solid Buoyancy Materials. Eng Technol Open Acc. 2020; 3(4): 555620. DOI: 10.19080/ETOAJ.2020.03.555620.

distribute along radial direction is discontinuous at interface. The radial normal stress at inner surface of the hollow glass bead is 0. Therefore, the tangential stress may be the main factor leading to the fracture of unit cell.

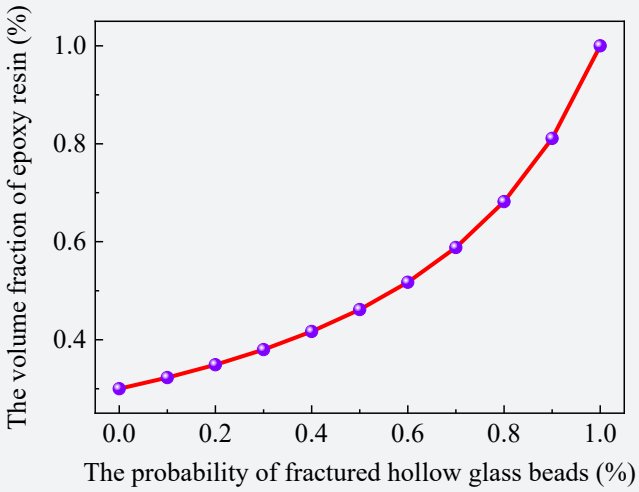

Figure 5: The volume fraction of epoxy resin increases changing with the fracture of hollow glass beads.

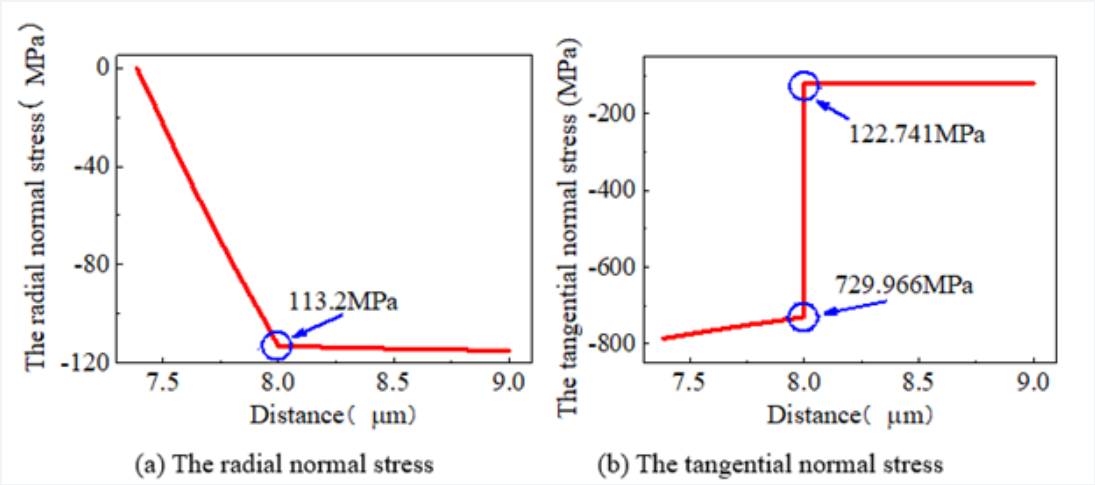

Figure 6: The radial and tangential normal stress distributions along radial direction.

The maximum shear stress distribution along radial direction is shown in Figure 7. It shows that the maximum shear stress occurs on the inner surface of hollow glass bead. The relationship between the maximum shear stress on the inner surface and the uniform pressure is shown in Figure 8. The curve in this figure is a straight line. In this paper, the slope of the line for the HZ-42 solid buoyancy material is k = 3.40.

Table 7: The uniform pressure and sizes of unit cell.

r_g(μm)	r_i(μm)	r_m(μm)	Uniform Pressure (MPa)
7.39	8	9	115

Compressive strength distribution

The compressive strength distribution of the unit cell is shown in Figure 9. It can be seen that the compressive strength does not follow the normal distribution through the asymmetry of the curve.

The crack section of solid buoyancy material under 165MPa pressure are shown in Figure 10. The compressive strength of unit cell decreases with the increase of particle size. Therefore, in

How to cite this article: Jingze W, Weicheng C. A Water Absorption Model Based on Self-Consistent Theory for Solid Buoyancy Materials. Eng Technol Open Acc. 2020; 3(4): 555620. DOI: 10.19080/ETOAJ.2020.03.555620.

theory, the hollow glass beads with larger particle sizes will fracture first. However, Figure 10 shows that the radii of hollow glass beads kept intact are generally small. It means that the compressive strength of unit cell is indeed related to the particle size. Figure 10 also shows that some hollow glass beads with smaller particle size also fractured. The reason for this phenomenon may be that the compressive strength of hollow glass beads with small particle size decreases due to defects.

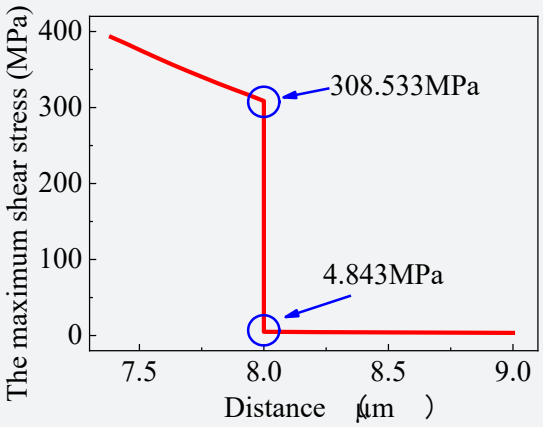

Figure 7: The maximum shear stress distribution along radial direction.

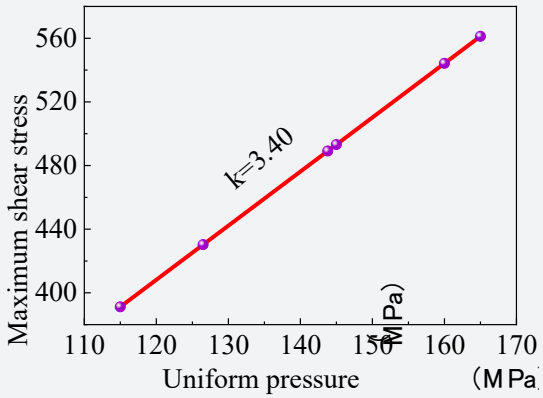

Figure 8: The relationship between the maximum shear stress and the uniform pressure.

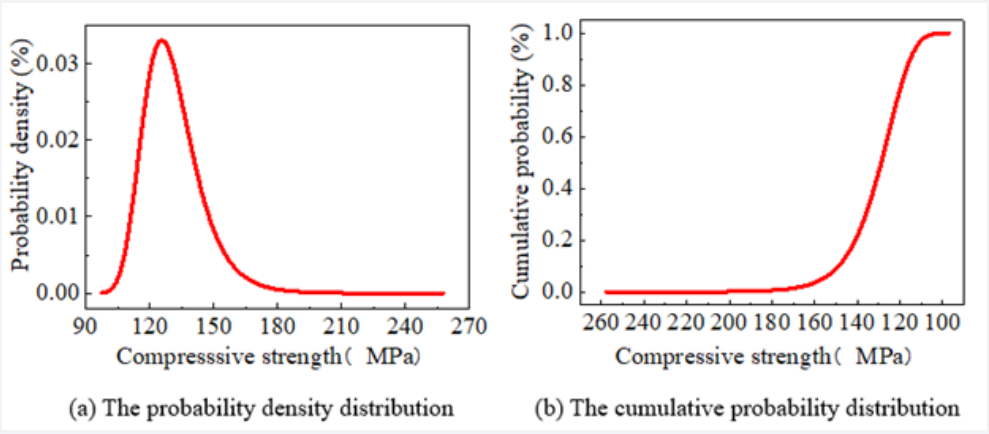

Figure 9: The compressive strength distributions of the unit cells.

How to cite this article: Jingze W, Weicheng C. A Water Absorption Model Based on Self-Consistent Theory for Solid Buoyancy Materials. Eng Technol Open Acc. 2020; 3(4): 555620. DOI: 10.19080/ETOAJ.2020.03.555620.

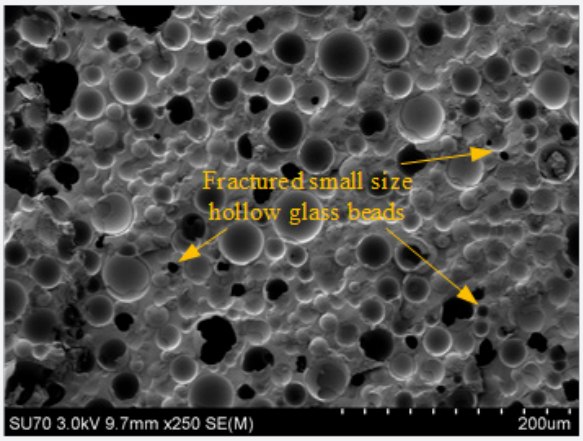

Figure 10: The crack section of solid buoyancy material.

Summary and Conclusion

A water absorption model based on self-consistent theory for solid buoyancy materials has been proposed after investigating the failure behavior of hollow glass beads. Then the water absorption model is verified by comparing with the experimental results. It shows that the failure of solid buoyancy materials is mainly caused by the fractured hollow glass beads. Therefore, the maximum shear stress is the dominant factor in the failure process of solid buoyancy materials. The crack sources in the solid buoyancy materials also occur on the inner surface of hollow glass beads.

The water absorption behavior of solid buoyancy materials is mainly caused by the fractured hollow glass beads. It can be divided into two stages. In the first stage, the water pressure is still low. The crack does not propagate after the hollow glass beads fracturing. On the other hand, due to the short time of testing time, the hollow part of the fractured glass beads cannot be completely filled with water. Therefore, it is assumed that the water absorption is directly proportional to the volume fraction of fractured hollow glass beads. In the second stage, the fragmentations of hollow glass beads propagate under a certain water pressure. Then the water absorption is exponentially related to the volume fraction of the fractured hollow glass beads. The water absorption model shows that, for the HZ-42 solid buoyancy material, the boundary between the first and the second stages is 128.4MPa.

It is shown that the fracture degree predicted by theory is severer than experimental results. Analysis shows that the deviation mainly comes from the volume fraction change during the fracture process of hollow glass beads. Increase of volume fraction makes the epoxy resin to share more pressure. This has not been considered in the model derivation process. Therefore, further study is required.

The distributions of stresses, compressive strength and volume has been investigated in this part. It can be seen that most of the radial and tangential normal stresses are borne by the hollow glass bead. The maximum shear stress occurs on the inner surface of hollow glass bead. The crack section of solid buoyancy material under 165MPa pressure shows that the radii of hollow glass beads kept intact are generally small. This proves that the compressive strengths of unit cells are related to its particle sizes. However, some hollow glass beads with small particle sizes also fractured. This phenomenon may be caused by the defects.

Acknowledgement

This work is supported by the General Program of National Natural Science Foundation of China 'Study on water absorption characteristics of buoyancy material in full ocean depth manned submersible' (Grant No.51879157), the National Natural Science Foundation of China for Youth Science Project 'Mechanism of stress-moisture-creep coupling on compressive strength of composites in deep-sea' (Grant No.11902288) and the "Construction of a Leading Innovation Team" project by the Hangzhou Municipal government.

References

1. Cui WC, Guo J, Pan BB (2018) A Preliminary Study on the Buoyancy Materials for the Use in Full Ocean Depth Manned Submersibles. Journal of Ship Mechanics 22(6): 736-757.
2. Endo M, Yokota K, Nanba N (1972) New Buoyancy Material for Deep Submersibles: 2nd Report. Journal of the Kansai Society of Naval Architects Japan 143:17-24.
3. Walden B, Tessier N, Popenoe H (2010) Newly developed specification and test methods for syntactic foam buoyancy material for deep ocean manned submersible vehicles. OCEANS 2010 MTS/IEEE SEATTLE.
4. Wang F, Wang K, Cui WC (2015) A simplified life estimation method for the spherical hull of deep manned submersibles. Marine Structures 44(4): 159-170.
5. Pan BB, Cui WC, Ye C, et al. (2012) Development of the unpowered diving and floating prediction system for deep manned submersible "JIAOLONG". Journal of Ship Mechanics 18(20): 2379-2385.

How to cite this article: Jingze W, Weicheng C. A Water Absorption Model Based on Self-Consistent Theory for Solid Buoyancy Materials. Eng Technol Open Acc. 2020; 3(4): 555620. DOI: 10.19080/ETOAJ.2020.03.555620.

6. Hobaica EC, Cook SD (1971) Composite buoyancy material. US Patent 3622437.
7. Feng WQ, Wei DZ, Xian C, et al (2005) Preparation and characterization of solid buoyancy materials based on epoxy resins. Fine Chemicals.
8. Chen YC, Li XH, Ma YQ, et al. (2018) Water Absorption and Compressibility of Solid Buoyancy Materials Based on Epoxy Resins. Physical Testing and Chemical Analysis (Part A: Physical Testing) (54).
9. Adamson MJ (1980) Thermal expansion and swelling of cured epoxy resin used in graphite/epoxy composite materials. Journal of Materials Science 15(7): 1736-1745.
10. Xiao GZ, Shanahan MER (2009) Swelling of DGEBA/DDA epoxy resin during hygrothermal ageing. Polymer 39(14): 3253-3260.
11. Lana B (2009) Influence of hydrolysis on properties of organic-inorganic hybrid materials based on epoxy resin. Hrvatska znanstvena bibliografija i MZOS-Svibor.
12. Fromonteil C, Bardelle P, Cansell F (2000) Hydrolysis and Oxidation of an Epoxy Resin in Sub- and Supercritical Water. Industrial & Engineering Chemistry Research 39(4): 922-925.
13. Le Gall M, Choqueuse D, Le Gac PY, Davis P, Perreux D (2014) Novel mechanical characterization method for deep sea buoyancy material under hydrostatic pressure. Polymer Testing 39: 36-44.
14. Zhao QX (2019) Determining the Damage Mechanisms for Buoyancy Materials of Deep-Sea Manned Submersibles. Journal of Coastal Research 35(5): 996-1002.
15. Bunn P, Mottram JT (1993) Manufacture and compression properties of syntactic foams. Composites 24(7): 565-571.
16. Devi KA, John B, Nair CPR, Ninan KN (2010) Syntactic foam composites of epoxy-allyl phenol-bismaleimide ternary blend—Processing and properties. Journal of Applied Polymer Science 105(6): 3715-3722.
17. Swetha C, Kumar R (2011) Quasi-static uni-axial compression behaviour of hollow glass microspheres/epoxy based syntactic foams. Materials & Design 32(8-9): 4152-4163.
18. Wouterson EM, Boey FYC, Hu X, Wong SC (2005) Specific properties and fracture toughness of syntactic foam: Effect of foam microstructures. Composites Science & Technology 65(11-12): 1840-1850.
19. Gupta N, Woldesenbet E, Mensah P (2004) Compression Properties of Syntactic Foams: Effect of Cenosphere Radius Ratio and Specimen Aspect Ratio. Composites Part A: Applied Science and Manufacturing 35(1): 103-111.
20. Woldesenbet E, Gupta N, Jerro HD (2005) Effect of Microballoon Radius Ratio on Syntactic Foam Core Sandwich Composites. Journal of Sandwich Structures & Materials 7(2): 95-111.
21. Nguyen NQ, Gupta N (2010) Analyzing the effect of fiber reinforcement on properties of syntactic foams. Materials Science & Engineering A 527(23): 6422-6428.
22. Kim HS, Plubrai P (2004) Manufacturing and failure mechanisms of syntactic foam under compression. Composites Part A Applied Science & Manufacturing 35(9): 1009-1015.
23. Liang JZ (2002) Tensile and Impact Properties of Hollow Glass Bead-Filled PVC Composites. Macromolecular Materials & Engineering 287(9): 588-591.
24. Liang JZ (2007) Impact fracture toughness of hollow glass bead-filled polypropylene composites. Journal of Materials Science 42(3): 841-846.
25. Liang JZ (2005) Mechanical Properties of Hollow Glass Bead-filled ABS Composites. Journal of Thermoplastic Composite Materials 18(5): 407-416.
26. Liang JZ (2006) Impact Fracture Behavior of Hollow Glass Bead-Filled ABS Composites. Journal of ASTM International 3(4): 1-7.
27. Chen YC, Li XH, Ma YQ, et al. (2018) Research Progress on Water Absorption of Epoxy Resin and Epoxy Resin Based Solid Buoyancy Materials. Physical Testing and Chemical Analysis (Part A: Physical Testing).
28. Sendova T, Walton JR (2010) The defect of surface tension in modeling interfacial fracture.
29. Cheng YC (1920) Cohesion, Adhesion, tensile strength, tensile energy, negative surface energy, interfacial tension, and molecular attraction.

DOI: 10.19080/ETOAJ.2020.03.555620

How to cite this article: Jingze W, Weicheng C. A Water Absorption Model Based on Self-Consistent Theory for Solid Buoyancy Materials. Eng Technol Open Acc. 2020; 3(4): 555620. DOI: 10.19080/ETOAJ.2020.03.555620.